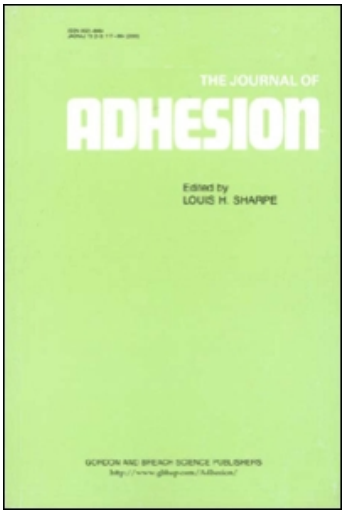

The Journal of Adhesion
Publication details, including instructions for authors and subscription information:
http://www.informaworld.com/smpp/title~content=t713453635

The Fatigue and Durability Behaviour of Automotive Adhesives. Part III: Predicting the Service Life

A. J. Curley[ab]; J. K. Jethwa[ac]; A. J. Kinloch[a]; A. C. Taylor[a]
[a] Department of Mechanical Engineering, Imperial College of Science, Technology and Medicine, London, UK [b] Kingston University, School of Computer Science and Electronic Systems, London, UK [c] Autoliv, Havant, Hampshire, UK

To cite this Article Curley, A. J. , Jethwa, J. K. , Kinloch, A. J. and Taylor, A. C.(1998) 'The Fatigue and Durability Behaviour of Automotive Adhesives. Part III: Predicting the Service Life', The Journal of Adhesion, 66: 1, 39 — 59
To link to this Article: DOI: 10.1080/00218469808009959
URL: http://dx.doi.org/10.1080/00218469808009959

J. Adhesion, 1998, Vol. 66, pp. 39–59
Reprints available directly from the publisher
Photocopying permitted by license only

The Fatigue and Durability Behaviour of Automotive Adhesives. Part III: Predicting the Service Life

A. J. CURLEY*, J. K. JETHWA**, A. J. KINLOCH† and A. C. TAYLOR

Department of Mechanical Engineering, Imperial College of Science, Technology and Medicine, Exhibition Rd., London, SW7 2BX, UK

(Received 16 June 1997; In final form 18 August 1997)

In Part I [1] a fracture mechanics approach has been successfully used to examine the cyclic fatigue behaviour of adhesively-bonded joints, which consisted of aluminium-alloy or electro-galvanised (EG) steel substrates bonded using toughened-epoxy structural paste-adhesives. The adhesive systems are typical of those being considered for use, or in use, for bonding load-bearing components in the automobile industry. The results were plotted in the form of the rate of crack growth per cycle, da/dN, *versus* the maximum strain-energy release-rate, G_{max}, applied in the fatigue cycle, using logarithmic axes. In Part II [2] the mechanisms of failure were considered, particularly the mechanisms of environmental attack. The present paper, Part III, discusses the use of the relationship between da/dN and G_{max}, which can be obtained in a relatively short timescale, to predict the fatigue lifetime of (uncracked) single-overlap joints cyclically loaded in tension. An analytical and a finite-element model have been derived to predict the number of cycles of failure, N_f, for lap joints and, particularly when the latter model was used to deduce the value of the strain-energy release-rate, G, in the lap joints, the agreement between the theoretical predictions and the experimental results is found to be very good.

Keywords: Aluminium alloy; automotive applications; fatigue; finite-element analysis; fracture mechanics; lifetime predictions; structural adhesives

*Present address: Kingston University, School of Computer Science and Electronic Systems, Penrhyn Rd., Kingston upon Thames, London, KT1 2EE, UK.
**Present address: Autoliv, Penner Rd., Havant, Hampshire, PO9 1QH, UK.
†Corresponding author.

1. INTRODUCTION

The present research is particularly directed towards adhesives for automotive applications. Adhesives are currently used in many areas in the manufacture of automobiles, but almost always either as sealant materials or in non-critical secondary structures. So far the use of adhesives in truly structural applications has been very limited. A major reason for this has been a concern about the fatigue and durability behaviour of bonded, structural components over the expected lifetime of the vehicle, especially since the adhesive joints must perform satisfactorily under service conditions which include dynamically-applied loads and exposure to hostile environments such as water, petrol, other organic solvents, etc. Also, in many instances of course, combinations of these conditions may be experienced.

In Part 1 [1] a linear-elastic fracture-mechanics (LEFM) approach has been successfully used to examine the cyclic fatigue behaviour of adhesively-bonded joints, which consisted of aluminium-alloy or electro-galvanised (EG) steel substrates bonded using toughened-epoxy structural paste-adhesives. The adhesive systems are typical of those being considered for use, or in use, for bonding load-bearing components in the automobile industry. The two adhesives employed were (i) a one-part epoxy-paste adhesive, Grade "XD4600" supplied by Ciba Polymers, UK: this adhesive had been especially developed for bonding aluminium alloys; and (ii) a one-part epoxy-paste, Grade "Terokal 4520-34" supplied by Teroson: this adhesive is currently being used to bond EG steel parts for the automobile industry. In the case of the aluminium-alloy, before bonding the substrates were either grit-blasted and solvent degreased, or subjected to a chromic-acid etch. In the case of the EG steel, the substrates were simply solvent degreased using 1,1,1 trichloroethane.

The cyclic fatigue results were plotted in the form of the rate of crack growth per cycle, da/dN, *versus* the maximum strain-energy release-rate, G_{max}, applied in the fatigue cycle, using logarithmic axes, and a typical plot is shown in Figure 1. Of particular interest was the presence of a threshold value of the strain-energy release-rate, G_{th}, applied in the fatigue cycle, below which fatigue crack growth was not observed to occur. The cyclic fatigue tests conducted in a relatively dry environment of 23°C and 55% r.h. were shown to cause crack

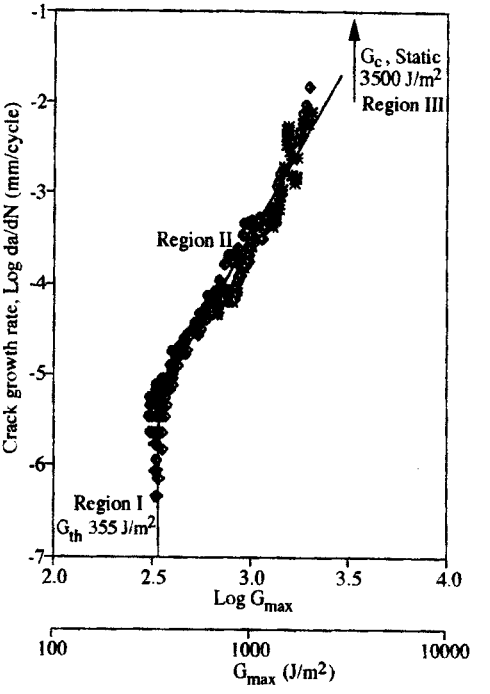

FIGURE 1 Logarithmic crack growth rate per cycle, *da/dN*, *versus* logarithmic, and linear, G_{max} for the aluminium-alloy/"XD4600" TDCB joints which were prepared using the chromic-acid etching pretreatment and were conducted in the "dry" environment of 23°C and 55% r.h.

propagation at far lower value of G_{max} compared with the values of the adhesive fracture energies, G_c, which were determined from monotonically-loaded fracture tests. Indeed, the value of the adhesive fracture energy, G_c, for the adhesive used to obtain the data given in Figure 1 was 3500 J/m^2. For the tests conducted in this relatively dry environment of 23°C and 55% r.h., the locus of joint failure was always *via* cohesive crack growth through the adhesive layer.

Cyclic fatigue tests were also conducted in a "wet" environment, namely immersion in distilled water at 28°C. The "wet" fatigue tests clearly revealed the further significant detrimental effect that a hostile environment may have upon the mechanical performance of adhesive joints, and highlighted the important influence that the surface

pretreatment, used for the substrates prior to bonding, has upon joint durability. In Part II [2] the locus of failure was identified and the mechanisms of environmental attack and failure were discussed in detail.

Apart from using such results as shown in Figure 1 to rank different adhesive "systems" (i.e., combinations of adhesive/substrate type/surface pretreatment), it is also of considerable interest to employ such data to try to predict the service-life of adhesive joints. This is potentially very rewarding, since the fracture-mechanics data may be gathered in a relatively short time-scale. Thus, if these data could be used to predict the *long-term* behaviour of various, possibly complex, designs of adhesive joints, then this would represent a major advance in increasing the design engineer's confidence in the use of adhesive bonding. Hence, in the present paper, Part III, the results presented in earlier papers will be used in an attempt to predict the fatigue lifetime of single-overlap joints, which were not precracked, subjected to cyclic fatigue loading.

2. EXPERIMENTAL

2.1. The Materials

For the present work, the substrate employed was an aluminium alloy (Grade: EN AW-5083) which contained 4.0 to 4.9% magnesium and 0.4 to 1.0% manganese. The adhesive employed was a one-part epoxy-paste adhesive, Grade "XD4600" supplied by Ciba Polymers, UK. This adhesive had been especially developed for bonding aluminium alloys.

2.2. Joint Preparation

The single-overlap joints conformed [3] to ASTM D1002. The thickness of the aluminium-alloy plate was 1.62 mm and the joints were 25.4 mm in width, with a bonded overlap of length 12.7 mm. Before bonding, the aluminium-alloy substrates were subjected to a surface treatment which consisted of a chromic-acid etch [4]. Steel wire, 0.4 mm in diameter, was used to control the thickness of the

adhesive layer. The adhesive was then cured by a two-stage heating process. The joints were initially placed in an oven pre-heated to 145°C for 10 minutes, after which the oven temperature was raised to 190°C. It took about 15 minutes for the oven to reach 190°C, when the heaters were switched off and the oven, and joints, were allowed to cool slowly overnight. A low pressure was applied to the joints during the adhesive curing process.

2.3. Joint Testing

To obtain values of the initial strength of the lap joints, monotonically-loaded tests were conducted at a displacement rate of 0.5 mm/min. The tests were conducted in the "dry" environment of 23 ± 1°C, and the relative humidity was 55%.

To obtain the fatigue life of the lap joints, values of the number, N_f, of cycles to failure for the lap joints were measured as a function of the maximum load, T_{max}, per unit width, applied in a fatigue cycle. A sinusoidal loading waveform was employed at frequency of 5Hz. A range of maximum loads, T_{max}, per unit width were employed and the load ratio ($=T_{min}/T_{max}$) was 0.5. The tests were conducted in the "dry" environment, with a test temperature of 23 ± 1°C and a relative humidity of 55%.

3. THEORETICAL

3.1. Introduction

To employ the fracture mechanics data (see, for example, Fig. 1) to predict the fatigue life of (nominally uncracked) adhesively-bonded joints, or adhesively-bonded components, the first step is to obtain an expression for the fracture mechanics data.

The second step is to derive a model for the total strain-energy release-rate, G, in the joint, or bonded component, of interest as a function the length of the fatigue crack, which is assumed to initiate and propagate through the joint, for the given joint geometry and type of loading applied.

In the third step, this model, giving G for the bonded component as a function of crack length for the given joint geometry and applied

loading, may then be combined with the expression for the *da/dN versus* G_{max} curve to give predictions of the long-term fatigue life of the joint or structure.

In the present work, both an analytical model, based upon a beam-theory approach [5], and a finite-element (FE) model [6] were used to model the second step. However, in the case of either the analytical or the FE model, the first step is to identify an expression to describe the typical fatigue curve when the rate of crack growth per cycle, *da/dN*, is plotted against the maximum strain-energy release-rate, G_{max}, applied in the fatigue cycle, as illustrated in Figure 1.

3.2. The Fracture-Mechanics Fatigue Curve

It is now well established that, over much of the range of experimental data, the fatigue crack growth rate, *da/dN*, may be expressed in the form of the Paris Law, where the value of *da/dN* is expressed as a function of the applied maximum strain-energy release-rate, G_{max}, as given below:

$$\frac{da}{dN} = DG_{max}^{n} \tag{1}$$

Here D and n are empirical constants for a given loading ratio, frequency of testing and environment.

However, the complete relationship between logarithmic G_{max} and *da/dN* is often of a sigmoidal form, as may be seen in Figure 1, which may be better expressed by [5, 7, 8]:

$$\frac{da}{dN} = DG_{max}^{n} \left\{ \frac{1 - \left(\frac{G_{th}}{G_{max}} \right)^{n_1}}{1 - \left(\frac{G_{max}}{G_c} \right)^{n_2}} \right\} \tag{2}$$

where G_{th} is the minimum or threshold value of the applied strain energy release-rate, below which no crack growth is observed to occur, and D, n, n_1, and n_2 are constants for a given set of test conditions.

It should be noted that G_{max} has been employed, as opposed to ΔG, since during the unloading part of the fatigue cycle the debonded surfaces typically come into contact, resulting in facial interference of

the adhesive with itself (if cohesive-in-the-adhesive failure occurs) or with the metal surface (if interfacial failure occurs). This leads to the generation of surface debris which prevents the crack from fully closing when it is unloaded, and hence may give an artificially high value of G_{min}. Thus, it has been suggested [5, 7, 8] that it is better to use G_{max}, instead of ΔG; and this convention has been followed in the present studies. However, the choice of this approach does not significantly affect the general form of the fatigue crack-growth relationships.

3.3. The Analytical Predictive Model

Obviously, to employ the fracture mechanics data generated from the above studies, the total strain-energy release-rate, G, *versus* the length of the propagating fatigue crack, a, in a single lap-joint during cyclic fatigue loading needs to be deduced. This relationship may then be substituted into Eq. (2), which can then be integrated to give the number of cycles to failure, N_f, as a function of the load, or stress, applied during the fatigue cycle. An analytical model to perform these tasks is described below, and follows that discussed in detail previously [5].

It is well documented [9] that single-overlap joints loaded in tension fail due to the transverse (out-of-plane) tensile, or cleavage, stresses, σ_{11}, which act at right angles to the direction of the applied load. These stresses are mainly introduced by the eccentricity of the loading path. Now, the maximum value of the transverse tensile stress, σ_{11}, in a lap joint is given by [10, 11].

$$\sigma_{11} = M_e \left(\frac{E_a}{2 t_a X} \right)^{1/2} \tag{3}$$

where E_a and t_a are the modulus and thickness of the adhesive layer, respectively. The bending stiffness, X, per unit width and the bending moment, M_e, per unit width are given by:

$$X = \frac{E_s h^3}{12(1 - \upsilon^2)} \tag{4}$$

and

$$M_e = 0.5KT(h + t_a) \tag{5}$$

where the bending moment factor, K, is given by:

$$K = \frac{1}{1 + \varepsilon c} \tag{6}$$

where

$$\varepsilon = \left(\frac{T}{X}\right)^{1/2} \tag{7}$$

and where E_s, h and υ are the modulus, thickness and Poisson's ratio of the substrate material, c is one-half of the bonded overlap length and T is the load per unit width applied to the lap joint.

Now a very powerful method for deducing the strain-energy release-rate acting in a cracked beam is based upon a knowledge of the bending moments at the crack tip. For symmetrical loading, the mode I strain-energy release-rate, G, is given [12].

$$G = \frac{12M_e^2}{E_s h^3} \tag{8}$$

Combining Eqs. (3–8), the value of $G_{\max}$ may be expressed by:

$$G_{\max} = \frac{12}{E_s h^3}\left(\frac{T_{\max}(h + t_a)}{2}\right)^2\left(\frac{1}{(1 + \varepsilon c)^2}\right) \tag{9}$$

where $T_{\max}$ is the load per unit width applied to the lap joint during a fatigue cycle. Assuming that the fatigue crack initiates and grows from each end of the bonded overlap, then the growth of the crack by a length, a, from either end will change the effective overlap length from $2c$ to $(2c - 2a)$. Thus, Eq. (9) will become:

$$G_{\max} = \frac{12}{E_s h^3}\left(\frac{T_{\max}(h + t_a)}{2}\right)^2\left(\frac{1}{(1 + \varepsilon[c - a])^2}\right) \tag{10}$$

The number of cycles to failure, N_f, of the single lap joint subjected to cyclic loading may be estimated by combining Eqs. (2) and (10), to eliminate $G_{\max}$, and then integrating between the limits of the initial flaw size, a_o, and the crack length, a_f, at which rapid fracture of the joint occurs. This gives:

$$N_f = \int_{a_o}^{a_f} \frac{[E_s h^3[1+e(c-a)]^2]^{n-n_2}}{DG_c^{n_2}[3[T_{\max}(h+t_a)]^2]^{n-n_1}} \times \left[\frac{[G_c E_s h^3[1+e(c-a)]^2]^{n_2} - [3[T_{\max}(h+t_a)]^2]^{n_2}}{[3[T_{\max}(h+t_a)]^2]^{n_1} - [G_{\text{th}} E_s h^3[1+e(c-a)]^2]^{n_1}}\right] da \tag{11}$$

In this equation the values of the fracture mechanics parameters (i.e., D, n, n_1, n_2, G_{th} and G_c) may be deduced from the fatigue data obtained from the fracture mechanics specimens. Further, the geometry of the single-lap joint whose fatigue behaviour is to be predicted is known and so the values of the parameters ε, h, t_a and c are known, as is the modulus, E_s, of the substrate materials forming the lap joint. Hence, if the values of the integration limits can be identified, then the number of cycles to failure, N_f, of the single lap joint may be predicted as a function of the maximum load per unit width, $T_{\max}$, of the joint applied during a fatigue cycle. The integration limits, a_0 and a_f, represent the initial (Griffith) flaw size and the length of the fatigue crack when fast fracture occurs, respectively, and may be readily calculated from the expressions:

$$a_0 = \frac{E_a G_c}{\pi \sigma_a^2} \tag{12}$$

where σ_a is the tensile strength of the adhesive. The length of the fatigue crack when fast, catastrophic, failure results may be determined by re-arranging Eq. (10) and letting $G_{\max} = G_c$:

$$a_f = c - \frac{1}{\varepsilon}\left(\left(\frac{3(T_{\max}[h+t_a])^2}{E_s h^3 G_c}\right)^{1/2} - 1\right) \tag{13}$$

where, obviously $a_f \leq c$.

3.4. The Finite-Element Predictive Model

3.4.1. The Basic FE Model

The total strain-energy release-rate, G, associated with the growth of a crack in the single-lap joint loaded in tension may also be deduced using a model based upon a finite-element (FE) analysis approach. FE models of adhesive joints have shown [9, 13] that high gradients of stress and strain exist in certain regions, especially near the adhesive/substrate interface. Now, the adhesive layer is very thin compared with the thickness of the substrates and to achieve reliable results it is necessary to use four or six elements through the thickness of the adhesive. A fine mesh, especially in the adhesive layer, will result in a relatively high accuracy in determining the stress field, but this will, of course, increase the number of degrees of freedom and result in increased computation time. However, it is possible to use a coarser mesh in the substrates outside of the bonded overlap region of the joint, and to position more elements nearer the adhesive layer. As a consequence, there are typically highly varying mesh-densities throughout the model, which complicates both pre-processing and post-processing of the analysis.

It is often possible to simplify the finite-element analysis of adhesive joints by using a two-dimensional model. In many joints, especially in relatively wide joints, the loading may be assumed to be in plane strain. This enables the problem to be reduced to a two-dimensional one, which significantly reduces the number of degrees of freedom and the necessary computation time. Fortunately, Adams and Peppiatt [14] have shown that the shear and tensile stress concentrations in the direction of the applied load are not significantly influenced by the transverse stresses caused by the Poisson's ratio strains in the substrates. This reveals that the use of three-dimensional elements, which would greatly increase the computation time, are not necessary.

In the present work, a two-dimensional (2D) analysis was, therefore, undertaken assuming plane-strain conditions. The ABAQUS code was used. The joints were modelled using four-noded quadrilateral 2D plane-strain, isoparametric, solid elements. Four elements were used through the thickness of the adhesive layer and six through the thickness of each substrate. The FE model required about 6000 degrees of freedom. The substrates and the adhesive were modelled as

elastic materials, and as separate parts which were linked together in the analysis. Along the interface pairs of nodes existed, one belonging to the adhesive and the other to the substrate. All degrees of freedom of the corresponding nodes were constrained to identical displacements. This enabled accurate determinations of the stresses at the interface caused by the large changes in stiffness between the different materials. The FE model took into account the changing geometry of the joint under the applied loading, which arises from rotation of the single-overlap joint. As for the analytical model described above, it will be assumed, in agreement with experimental observations [15, 16], that the fatigue cracks are located in the adhesive layer, and initiate at the ends of the overlap, propagating towards the centre.

3.4.2. Evaluation of the Strain-Energy Release-Rate, G

The value of strain-energy release-rate, G, may be calculated either locally or globally for a crack of length, a, and for a given applied load, T_{max}, acting on the lap joint. Both FE model methods were found to give a very similar result for the values of the strain-energy release-rate, G.

The Virtual Crack Closure Method The local approach employed the virtual crack closure method to calculate the value of strain-energy release rates. This method was developed by Rybicki and Kanninen [6] and uses the displacements and forces in the vicinity of the crack tip to calculate the strain-energy release-rate, G. It is based upon the argument that the strain energy required to extend a crack by small amount, Δ_a, is equal to the energy required to close the crack to its original dimensions. Thus, when used with a FE approach, the nodal values of force and displacement are used.

Figure 2 shows schematically the FE mesh near the crack tip and the notation used. The mode I and mode II values of the total strain-energy release-rates (i.e., G_I and G_{II}, respectively) may be deduced from the expressions given below, and the total value of the strain-energy release-rate, G, is simply the sum of these two contributions:

$$G_I = \lim(\Delta_a \to 0) \frac{1}{2\Delta_a} F_a(v_c - v_d) \tag{14a}$$

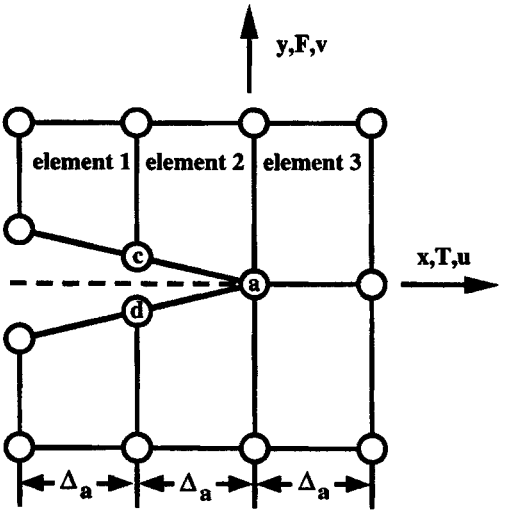

FIGURE 2 The finite element mesh around the crack tip.

$$G_{II} = \lim(\Delta_a \to 0)\frac{1}{2\Delta_a} T_a(u_c - u_d) \tag{14b}$$

where F_a and T_a represent the forces acting to hold the crack-tip closed, and v and u represent the displacements of the nodes immediately behind the crack tip (nodes "c" and "d"), in the directions shown in Figure 2.

It should be noted that this FE method does give the values of the individual contributions to the mode I and mode II components to the total strain-energy release-rate, G. However, we have simply summed these contributions to give the total strain-energy release-rate, G, since it has been shown [17, 18] that for relatively ductile adhesives, such as that used in the present work, the driving parameter for cyclic debonding is the total value of the strain-energy release-rate, G, rather than any individual component.

The value of the strain-energy release-rate, G, as a function of the joint geometry and loading conditions may also be deduced using the J-integral method.

The J-Integral Method The global approach which we employed [19] was the *J*-integral method implemented in the ABAQUS package, which was also proposed by Rybicki and Kanninen [6]. This method allows an integration path, taken sufficiently far from the crack tip, to be substituted for a path close to the crack tip regions. Therefore, it is possible to calculate the value of G for different crack lengths and applied loads.

A domain integral method was used to evaluate the *J*-integral around the crack tip [6, 19]. This method was found to be quite robust, in the sense that accurate *J*-integral estimates could be obtained with quite coarse meshes. This is because the integral is taken over a domain of elements surrounding the crack tip, so that errors in local solution parameters have a lesser effect. The *J*-integral method should be path-independent and any variation in *J*-integral values calculated on different contours would imply an inaccuracy in the model. In the present work, the *J*-integral method was indeed found to be path-independent, and there were no significant differences in the values of G which were deduced from the two different approaches.

3.4.3. Evaluation of G_{max}

The theoretical relationship between G_{max} and T_{max} from the FE modelling of cracks of various lengths in the single-lap joint loaded in tension is shown in Figure 3. (As commented previously, we found no significant differences in the results from employing either of the two different FE methods described above).

As shown in Figure 3, the relationship between G_{max} and T_{max} for a given crack length, a, is linear when the values of G_{max} are plotted versus T^2_{max} and, assuming that a LEFM approach is valid, this is indeed as expected (see for example Eqs. (8) or (9)). The variation of the slope, β, of the relationship between G_{max} and T^2_{max}, as a function of crack length, a, is shown in Figure 4. The relationship between the slope, β, and the crack length, a, may be represented by an exponential equation of the form:

$$\beta = \frac{G_{max}}{T^2_{max}} = 8.37 * 10^{-9} * 10^{100.61a} \tag{15}$$

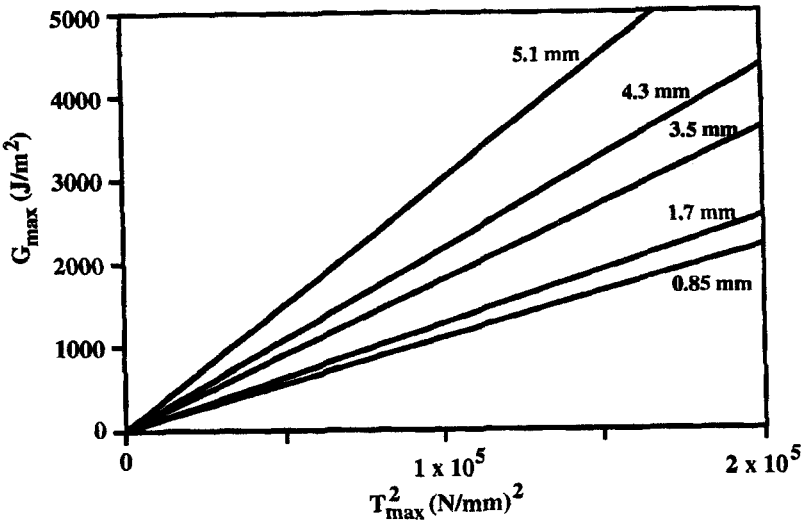

FIGURE 3 The relationships between G_{max} and T^2_{max} from the FE modelling for cracks of various lengths, a, in the single-lap joint loaded in tension.

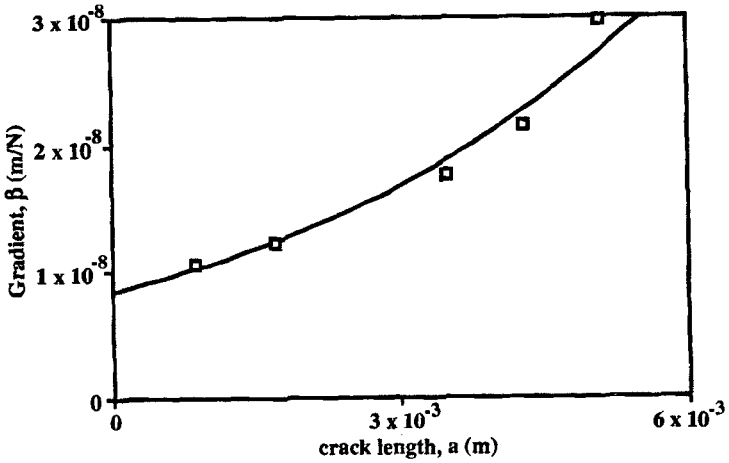

FIGURE 4 The relationship between the slope, β, (from the plots of G_{max} and T^2_{max}; see Fig. 3) and the crack length, a, in a single-lap joint loaded in tension from the FE modelling. (The solid line represents an exponential fit to the points, see Eq. (15)).

(However, it should be noted that a third-order polynomial expression also provides an excellent fit to the data shown in Fig. 4).

The above Eq. (15) may be substituted to Eq. (2) to eliminate the term G_{max}. This substituted version of Eq. (2) may then be integrated between the initial and final crack lengths to obtain the value of the number of cycles, N_f, to failure as a function of T_{max}. We performed [20] this integration using a computer software package ("Mathcad") which splits the integral into two intervals and uses the trapezium rule to calculate the value of N_f. Each interval is then split into half again and a new value of N_f is found. This process is repeated until two consecutive values of N_f differ by less than a specified tolerance. The default tolerance used was normally 10^{-3} cycles, although for calculations near the threshold value this was increased to a value of 1 cycle to reduce the calculation time.

4. RESULTS

4.1. Material and Joint Characterisation

The values of the constants employed in Eq. (2) to describe the fatigue behaviour for the "XD4600" adhesive/aluminium-alloy joints were obtained by fitting Eq. (2) to the results shown in Figure 1. The values are given in Table I.

The relevant properties of the adhesive material and the aluminium-alloy substrates are shown in Table II. These properties were used in the analytical and finite-element models, as described in the previous

TABLE I Fracture-mechanics fatigue data

Property	*Symbol and units*	*Value*
Adhesive fracture energy	G_c (J/m^2)	3500
Strain-energy release-rate at threshold	G_{th} (J/m^2)	355
Modified Paris Law coefficient	D	5.86×10^{-18}
Modified Paris Law exponent	n	3.54
Curve fitting constant at threshold	n_1	16 0
Curve fitting constant for the fast fracture region	n_2	0.46

Note: For the values of D, n, n_1 and n_2, the units of da/dN and G_{max} are m/cycle and J/m^2, respectively.

TABLE II Properties of the adhesive and aluminium-alloy substrates

Property	*Symbol and units*	*Value*
Modulus of the adhesive	E_a (GPa)	3.4
Fracture energy of the adhesive	G_c (J/m^2)	3500
Fracture stress of the adhesive[a]	σ_a (MPa)	97
Griffith flaw size of the adhesive[b]	a_0 (μm)	405
Fracture stress of the adhesive[c]	σ_a (MPa)	60
Griffith flaw size of the adhesive[d]	a_0 (μm)	1050
Modulus of the aluminium alloy	E_s (GPa)	71
Poisson's ratio of the aluminium alloy	ν	0.3

[a]Obtained *via* Eqs. (3) to (7) using the average failure load, T_c, per unit width for the single-lap joints of 443.8 N/mm.
[b]Obtained *via* using σ_a = 97 MPa and from Eq. (12).
[c]Obtained from tensile tests on the bulk adhesive.
[d]Obtained *via* using σ_a = 60 MPa and from Eq. (12).

section. It should be noted that two values for the fracture stress, σ_a, of the adhesive were considered, and these may be taken to represent upper and lower bound values. One value for σ_a may be deduced *via* Eqs. (3) to (7) using the average failure load, T_c, per unit width for the single-lap joints of 443.8 N/mm. This represents the fracture stress for the thin layer of adhesive *in-situ* in the adhesive joint. A lower bound value may be determined by conducting uniaxial tensile tests on specimens of the bulk adhesive; where, clearly, the chance of larger flaws in the specimens is greater, as there is a greater volume of adhesive being tested. Now, these two approaches yield values for σ_a of 97 and 60 MPa, respectively, and these values may now be used in Eq. (12) to deduce upper and lower bound values for the intrinsic flaw size, a_0. These values for the intrinsic flaw size, a_0, are also given in Table II.

4.2. The Single-Overlap Joints

The details of the geometry of the single-lap joint are shown in Table III. These values were used in the analytical and finite-element models, as described in the previous section. When monotonically loaded at a rate of 0.5 mm/min, the average failure load, T_c, per unit width for the single-lap joints was 443.8 N/mm, and this gives an average fracture stress, τ_c, for the lap joints of 34.9 MPa. The locus of failure for the lap joints was *via* cohesive fracture through the adhesive layer.

TABLE III Details of single-overlap joints

Property	*Symbol and units*	*Value*
Fracture stress[a]	τ_c (MPa)	34.9
Adhesive layer thickness	t_a (mm)	0.4
Substrate thickness	h (mm)	1.62
Half the bonded overlap length	c (mm)	6.35

[a] Tests were conducted at a rate of 0.5 mm/min and the coefficient of variation was ±4%.

4.3. Fatigue Behaviour of Single-Overlap Joints

The results for the fatigue behaviour of the single-lap joints are shown in Figure 5, and also in Figure 6. In these fatigue tests, the value of the number, N_f, of cycles to failure for the lap joints was measured as a function of the maximum load, T_{max}, per unit width applied in a fatigue cycle. A sinusoidal loading waveform was employed at a frequency of 5Hz. A range of maximum loads per unit width, T_{max}, were employed and the load ratio ($=T_{min}/T_{max}$) was 0.5. The tests were conducted in the dry environment, with a test temperature of 23 ± 1°C and a relative humidity of 55%.

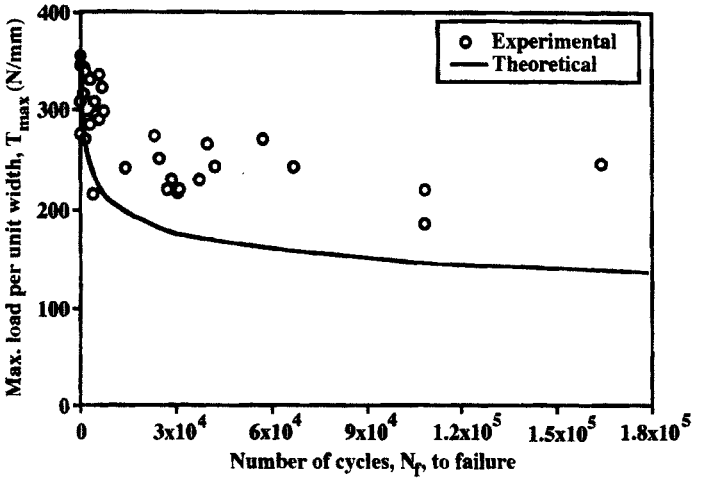

FIGURE 5 The number, N_f, of cycles to failure for the lap joints as a function of the maximum load, T_{max}, per unit width applied in a fatigue cycle. The points represent the experimental results whilst the solid line is the predicted theoretical relationship using the analytical model.

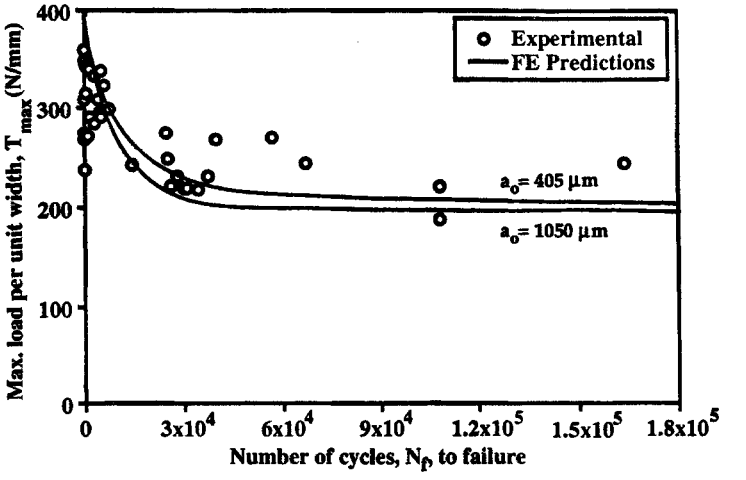

FIGURE 6 The number, N_f, of cycles to failure for the lap joints as a function of the maximum load, T_{max}, per unit width applied in a fatigue cycle. The points represent experimental results whilst the solid lines are predicted theoretical relationships using the FE model for a_0 values of 405 μm or 1050 μm, as indicated.

For the results shown in these figures, the locus of failure for the joints was always *via* a cohesive fracture through the adhesive layer. However, it was found that if values of T_{max} of lower than about 200 N/mm were employed, then failure of the lap joint occurred in the aluminium-alloy substrate. The aluminium-alloy substrates were polished in an attempt to overcome this problem, but to no avail. Thus, these observations lead to a value of T_{max} of about 200 N/mm representing the lowest limit at which we could obtain failure in the adhesive layer upon fatigue testing. It is of interest to note that this value of T_{max} represents about 45% of the fracture value, T_c, obtained from a monotonic loading test. Also, it is noteworthy that, since we observe failure in the aluminium-alloy substrates at fatigue loads lower than this value, this observation of the change in the locus of failure is a very convincing demonstration of the excellent fatigue properties that one may obtain from modern structural adhesives.

It will be recalled that for the fracture-mechanics fatigue tests (see Fig. 1) the locus of joint failure is through the adhesive layer. As noted above, this is also the case for crack growth in the fatigue tests on the

single-lap joints, provided these tests are conducted at relatively high fatigue loads, which results in fatigue lifetimes, N_f, up to about 2×10^5 cycles to failure. Therefore, clearly, this is the regime over which the accuracy of the predictions from the two theoretical lifetime models can be examined.

4.4. Predictions of Lifetime: Analytical Model

The results from using the analytical model, i.e., Eq. (11), for deducing the number, N_f, of cycles to failure for the lap joints as a function of the maximum load, T_{max}, per unit width applied in a fatigue cycle are shown in Figure 5. As may be seen, the agreement between the theoretical and experimental results is relatively poor. The analytical model used in Figure 5 employed in a value of a_0 of 405 μm, but the theoretical predictions would have been very similar if, instead, the value of a_0 had been taken to be 1050 μm (see Tab. II).

The relatively poor agreement seen in Figure 5 between the experimental results and the theoretical predictions is in direct contrast to the good agreement seen in previous work [5]. However, in the previous work the substrates were carbon-fibre epoxy composites. Unlike the aluminium-alloy substrates used in the present studies, these composite substrates would not have undergone any significant rotation and bending at the ends of the bonded overlap. Since such factors are not accounted for in the analytical model, this may possibly be the reason why this model gives such a relatively poor prediction of the experimental results in the present work.

4.5. Predictions of Lifetime: Finite-Element Model

The results from using the finite-element model for deducing the number, N_f, of cycles to failure for the lap joints as a function of the maximum load, T_{max}, per unit width applied in a fatigue cycle are shown in Figure 6. There are several noteworthy points. Firstly, the finite-element model used in Figure 6 employed a value of a_0 of 405 μm. However, as in the case of the analytical model, the theoretical predictions are not very sensitive to the choice of the value of a_0; and virtually identical predictions would have been obtained had a value of a_0 of 1050 μm been used instead, as shown in Figure 6. Secondly, the

agreement between the theoretical and experimental results is very good. Thirdly, it is noteworthy that in the predictive models there is no allowance for an "initiation phase", and it appears that no such allowance is needed in order to obtain accurate predictions of the fatigue lifetime of the lap joints. This observation is in agreement with experimental work [16] which has revealed that fatigue cracks develop and begin to propagate through the adhesive layer in a single-lap joint, from the ends of the bonded region, without any significant initiation time being recorded. Fourthly, as a matter of interest, if the predictive model is run to give a value of N_f of 10^7cycles, then the predicted value of the required maximum fatigue load is about 40% of the value measured under monotonic loading.

It would clearly be very valuable to re-design the lap joint, and/or change the test conditions, so that the lap joints could be tested to give higher values of N_f, whilst maintaining failure through the adhesive layer. This would then enable the predictive models to be still applicable, and be an even more demanding test of the accuracy of the predictive modelling work. Such work is currently underway.

5. CONCLUSIONS

We have modelled the relationship between the number, N_f, of cycles to failure for adhesively-bonded single-overlap joints as a function of the maximum load, T_{max}, per unit width applied in a fatigue cycle, over which the failure mode was the same as that seen in the fracture-mechanics fatigue tests, i.e., cohesive through the adhesive layer. In the models all the various parameters may be directly measured or explicitly calculated. From Figure 6 it may be seen that the use of the finite-element model gives excellent agreement with the experimental results.

Finally, in considering the use of the present modelling work for adhesively-bonded components and structures, it should be noted that, in comparison with metallic materials, the value of the exponent "n" in Eqs. (1) or (2) for polymeric adhesives may be relatively high. This implies that for adhesives the rate of fatigue crack growth may rapidly increase for relatively small increases in the applied strain-energy release-rate, G_{max}. Thus, it may be argued that predicting a lower-

limit, threshold, load (below which fatigue crack growth will not be observed) is a better design philosophy in the case of adhesively-bonded joints and components. The present models are capable of predicting such a lower-limit value of T_{max} for the lap joints, and, indeed, in principle for any bonded joint or component, and current work is exploring the accuracy and usefulness of such modelling.

Acknowledgements

The authors are pleased to acknowledge the support and sponsorship of this work by the Ford Motor Company and the EPSRC. We would particularly like to acknowledge the assistance of Dr. R. Dickie, Mr. P. A. Fay and Mr. R. E. Davis.

References

[1] Jethwa, J. K. and Kinloch, A. J., *J. Adhesion* **61**, 71 (1997).
[2] Dickie, R. A., Haack, L. P., Jethwa, J. K., Kinloch, A. J. and Watts, J. F., *J. Adhesion.*
[3] ASTM, *Standard Test Method for Strength Properties of Adhesives in Shear by Tension Loading* **D 1002** (1983).
[4] Ministry of Defence, *Defence Specification*, UK 03–2/1 (1970).
[5] Kinloch, A. J. and Osiyemi, S. O., *J. Adhesion* **43**, 79 (1993).
[6] Rybicki, E. F. and Kanninen, M. F., *Engng. Fracture Mechs.* **9**, 931 (1977).
[7] Martin, R. H. and Murri, G. B., *ASTM STP* **1059**, 251 (1990).
[8] Osiyemi, S. O., *The Fatigue Performance of Adhesively Bonded Fibre-Composite Joints* (Ph.D Thesis, Univ. of London, 1992).
[9] Kinloch, A. J., *Adhesion and Adhesives: Science and Technology* (Chapman and Hall, London, 1983).
[10] Hart-Smith, L. J., *ASTM STP* **876**, 238 (1985).
[11] Zhao, X., Adams, R. D. and Pavier, M. J., in *Conference Proc. of Adhesion* '90, (Plastics and Rubber Institute, London, 1990), p. 35/1.
[12] Williams, J. G., *Int. J. Fracture* **36**, 101 (1988).
[13] Adams, R. D. and Wake, W. C., *Structural Adhesive Joints in Engineering* (Elsevier Applied Science, London, 1984).
[14] Adams, R. D. and Peppiatt, N. A., *J. Strain Analysis* **9**, 185 (1974).
[15] Gilchrist, M. and Smith, R. A., *J. Adhesion* **42**, 179 (1993).
[16] Fernando, M. and Kinloch, A. J., To be published.
[17] Johnson, W. S. and Mall, S., *ASTM STP* **876**, 189 (1985).
[18] Mall, S. and Kochhar, N. K., *Engng. Fracture Mechs.* **31**, 747 (1988).
[19] Judge, R. C. B. and Marsden, B. J., *NAFEMS*, National Engineering Laboratory, UK, Paper R0028 (1993).
[20] Taylor, A. C., *The Impact and Durability Performance of Adhesively-Bonded Metal Joints* (Ph.D Thesis, Univ. of London, 1997).